Entanglement entropy and Schmidt number as measures of delocalization of α clusters in one-dimensional nuclear systems

AUTHOR(S):

Kanada-En'yo, Yoshiko

CITATION:

Kanada-En'yo, Yoshiko. Entanglement entropy and Schmidt number as measures of delocalization of α clusters in one-dimensional nuclear systems. Progress of Theoretical and Experimental Physics 2015, 2015(4): 043D04.

ISSUE DATE:

2015-04

URL:

http://hdl.handle.net/2433/216699

PTEP
Prog. Theor. Exp. Phys. **2015**, 043D04 (20 pages)
DOI: 10.1093/ptep/ptv050

Entanglement entropy and Schmidt number as measures of delocalization of α clusters in one-dimensional nuclear systems

Yoshiko Kanada-En'yo*

Department of Physics, Kyoto University, Kyoto 606-8502, Japan
*E-mail: yenyo@ruby.scphys.kyoto-u.ac.jp

Received January 27, 2015; Revised February 27, 2015; Accepted March 14, 2015; Published April 23, 2015

We calculate the von Neumann entanglement entropy and the Schmidt number of one-dimensional (1D) cluster states and show that these are useful measures to estimate entanglement caused by delocalization of clusters. We analyze system size dependence of these entanglement measures in the linear-chain $n\alpha$ states given by Tohsaki–Horiuchi–Schuck–Röpke wave functions for 1D cluster gas states. We show that the Schmidt number is an almost equivalent measure to the von Neumann entanglement entropy when the delocalization of clusters occurs in the entire system but it shows different behaviors in a partially delocalized state containing localized clusters and delocalized ones. Thus the Rényi-2 entanglement entropy, which relates to the Schmidt number, is found to be almost equivalent to the von Neumann entanglement entropy for the full delocalized cluster system but it is less sensitive to the partially delocalized cluster system than the von Neumann entanglement entropy. We also propose a new entanglement measure which is a generalized form of the Schmidt number. The sensitivity of these measures of entanglement to the delocalization of clusters in low-density regions is discussed.

Subject Index D10

1. Introduction

Nuclear many-body systems are self-bound systems of four species of fermions, spin up and down protons, and neutrons. There, a variety of phenomena arise originating in many-body correlations. One of the remarkable spatial correlations is "cluster" which is a subunit composed of strongly correlating nucleons. A typical cluster in nuclear systems is an α cluster, which is a composite particle consisting of four nucleons. If there is no correlation between nucleons in a nucleus, all nucleons behave as independent particles and the nucleus is an uncorrelated state with a clear Fermi surface written by a single Slater determinant wave function. However, in reality, correlations between nucleons are rather strong and α clusters are often formed at the surface, in particular in light nuclei. Once α clusters are formed, delocalization of clusters occurs to reduce the kinetic energy of the center of mass motion (c.m.m.) of clusters in some situations. The delocalization of clusters involves many-body correlations beyond a Slater determinant. Note that a single Slater determinant contains the trivial correlation because of the antisymmetrization of nucleons. However, our interest in this paper is so-called quantum "entanglement," which is many-body correlations different from the trivial correlation. We focus on the many-body correlations caused by the delocalization of clusters, which is a kind of entanglement.

In realistic nuclear systems, a degree of the (de)localization of clusters depends on the competition (balance) of the kinetic energy and potential energy of clusters and is strongly affected also by the Pauli blocking between nucleons in clusters and a core nucleus. The delocalization limit of α clusters is an α cluster gas state, where all α clusters move almost freely like a gas. Such a cluster gas has been predicted to appear in the second 0^+ state of ^{12}C [1,2]. To describe cluster states of delocalized α clusters, a new type of cluster wave function, the so-called "Tohsaki–Horiuchi–Schuck–Röpke" (THSR) wave function, has been introduced by Tohsaki et al. [2]. The THSR wave function is essentially based on α clusters in a common Gaussian orbit having a range of the system size, and is suitable to describe general cluster gas states of $n\alpha$ clusters. Indeed, it has been shown that ^{8}Be(0^+_1) and ^{12}C(0^+_2) can be described well by the THSR wave functions of 2α and 3α, respectively. Since the optimized THSR wave functions for these states have much larger ranges of the Gaussian orbit of clusters than the cluster size, ^{8}Be(0^+_1) and ^{12}C(0^+_2) are interpreted as gas-like cluster states of 2α and 3α [2–5].

The THSR wave function has been extended to be applied to ^{20}Ne, and was also found to be able to describe ^{16}O+α states in ^{20}Ne [6,7]. Recently, Suhara et al. have proposed that this concept of the α-cluster gas is also applicable to one-dimensional (1D) cluster motion in linear-chain $n\alpha$ structures [8]. They have proposed 1D-THSR wave functions and shown that the 1D-THSR wave functions with optimized Gaussian ranges can describe well the exact solutions of linear-chain 3α and 4α states. Their result somewhat contradicts the the conventional picture of linear-chain $n\alpha$ structures, that spatially localized α clusters are arranged in 1D with certain intervals [9]. Even though their model restricted in 1D is not enough to settle the problem of stability of the linear-chain states in realistic nuclear systems in 3D, their work provides a new picture of 1D cluster states and may lead to an understanding of cluster phenomena in nuclear many-body systems. Moreover, the 1D cluster state is an academically interesting problem of quantum many-fermion systems.

To distinguish between localization and delocalization of composite particles (clusters) in microscopic wave functions of fermion (nucleon) systems, one should carefully consider the antisymmetrization effect of nucleons between clusters since any fermion system contains the trivial correlations because of the Pauli blocking, which are not our concern in this paper. When clusters largely overlap with each other, the motion of clusters is strongly affected by the Pauli blocking between nucleons in other clusters. As a result of the Pauli blocking effect, when the system size is as small as or smaller than the cluster size, clusters cannot move freely and the system becomes equivalent to a localized cluster state. In the case of a large system size, where the overlap between clusters is small, clusters can move rather more freely. It means that the delocalization occurs not in high-density regions but in low-density regions. Indeed, we have investigated the cluster motion of an α cluster around ^{16}O and shown that the delocalization of the cluster occurs in a long tail part far from the core [10]. Also in the 1D $n\alpha$ states, Suhara et al. have shown peak structures in the density distributions of the linear-chain 3α and 4α states, suggesting partial localization at high-density inner regions even in the 1D gases of 3α and 4α.

To estimate the many-body correlations caused by the delocalization of clusters, a kind of entanglement, we need a measure of correlations with which we can estimate the many-body correlations different from the trivial correlations because of antisymmetrization. There are several entanglement measures that are essentially based on the density matrix and can be used to estimate many-body correlations in quantum many-body systems. The Schmidt number [11] is one of the measures, and the von Neumann entanglement entropy [12] is another. The former was proposed by Grobe et al. in 1994 [11], and applied to measure entanglement, i.e., many-body correlations in such systems

as atomic and nuclear systems (see, for example, Refs. [13–15] and references therein). The latter was introduced by Bennett et al. in 1996 [12], and widely used in various fields such as condensed matter and quantum field theory (see Refs. [16–21] and references therein). General discussions of the quantum entanglement of composite particles such as hydrogen atoms are given in those references and also in Refs. [22–24]. In a previous paper, we have calculated the entanglement entropy for the one-body density matrix in 1D cluster states to measure the entanglement (correlations) caused by the delocalization of clusters, and found that the delocalization occurs in low-density regions but is relatively suppressed in high-density regions [25].

Let us consider uncorrelated and correlated states of fermion systems. An uncorrelated state is given by a Slater determinant wave function, for which the one-body density matrix $\hat{\rho}$ is a projector $\hat{\rho}^2 = \hat{\rho}$ in the single-particle Hilbert space. This means that the eigenvalues ρ_l of the one-body density matrix satisfy $\rho_l^2 = \rho_l$, i.e., $\rho_l = 1$ or 0. ρ_l is the occupation probability of the single-particle basis that diagonalizes the one-body density matrix and it is nothing but the Schmidt coefficients in the Schmidt decomposition for the one-body density matrix. Both the Schmidt number and entanglement entropy are entanglement measures which can estimate how the Schmidt coefficients deviate from the condition $\rho_l^2 = \rho_l$ for uncorrelated states. However, these measures have different dependencies on the one-body density matrix, i.e., the eigenvalues ρ_l.

In this paper, we calculate the entanglement entropy and the Schmidt number of 1D cluster states and make it clear whether these entanglement measures are useful to investigate the delocalization of clusters. We analyze the system size dependence of these measures in 1D α-cluster states given by the 1D-THSR wave functions. We show that the entanglement entropy and the Schmidt number are almost equivalent measures when the delocalization of clusters occurs in the entire system but they show different behaviors in partially delocalized cluster states composed of localized clusters and delocalized ones. We also propose a new entanglement measure which has a generalized form of the Schmidt number.

This paper is organized as follows. We describe the entanglement measures defined by the one-body density matrix in Sect. 2. Section 3 discusses properties of these measures of ideal states in a toy model. In Sect. 4, we calculate these measures in 1D nuclear systems of α clusters and discuss the sensitivity of these measures to the delocalization of clusters. The paper concludes with a summary in Sect. 5.

2. Measures of entanglement

The entanglement entropy and Schmidt number are the measures of entanglement in quantum many-body systems which are defined by the density matrix. In this section, we describe these measures and also propose a new measure by extending the Schmidt number. We also define spatial distributions of these entanglement measures.

2.1. One-body density matrix

In the present paper, we use only the one-body density matrix, which has often been discussed in nuclear systems [26], though more general density matrices are used to define measures of entanglement. For a wave function $|\Psi^{(A)}\rangle$ of an A-particle state, the matrix element of the one-body density in an arbitrary basis is given as

$$\rho_{pq} = \langle \Psi^{(A)} | c_q^\dagger c_p | \Psi^{(A)} \rangle, \tag{1}$$

where $c_p^\dagger$ and c_p are the creation and annihilation operators, respectively. The one-body density matrix is regarded as the matrix element of the one-body density operator $\hat{\rho}_\Psi$ for the wave function $\Psi^{(A)}$,

$$\hat{\rho}_\Psi| = \sum_{pq} |p\rangle \rho_{pq} \langle q|. \tag{2}$$

The one-body density matrix can be diagonalized by a unitary transformation of single-particle basis

$$\left(D^\dagger \rho D\right)_{ll'} = \rho_l \delta_{ll'}, \tag{3}$$

$$a_l^\dagger = \sum_{l'} D_{l'l} c_{l'}^\dagger, \tag{4}$$

where

$$\rho_l = \left\langle \Psi^{(A)} | a_l^\dagger a_l | \Psi^{(A)} \right\rangle, \tag{5}$$

$$0 \le \rho_l \le 1 \tag{6}$$

is the eigenvalue of the one-body density matrix and means the occupation probability of the single-particle state l in the wave function $\Psi^{(A)}$. ρ_l corresponds to so-called Schmidt coefficients in the Schmidt decomposition for the one-body density matrix. The trace of the one-body density matrix ρ equals the particle number A as

$$A = \mathrm{Tr}\rho = \sum_l \rho_l. \tag{7}$$

Note that the normalization of the one-body density matrix is not a unit but is the particle number A. In the present paper, the entanglement entropy and the Schmidt number are defined by the thus-defined one-body density matrix normalized as $\mathrm{Tr}\rho = A$.

If a wave function $|\Psi^{(A)}\rangle$ is a Slater determinant, $\rho_l = 1$ for occupied single-particle states and $\rho_l = 0$ for unoccupied single-particle states. This means that the one-body density operator $\hat{\rho}_\Psi$ satisfies $\hat{\rho}_\Psi^2 = \hat{\rho}_\Psi$ and is a projector in the single-particle Hilbert space if $\Psi^{(A)}$ is a non-entangled state given by a Slater determinant wave function.

2.2. *Measures of entanglement*

2.2.1. *Entanglement entropy*

The von Neumann entanglement entropy was introduced by Bennett et al. and proved to be an entanglement measure in quantum many-body systems (see, for instance, Refs. [15,18] and references therein). The entanglement entropy is defined by the von Neumann entropy of one of the reduced density matrices and is called "von Neumann entanglement entropy," which we call the "entanglement entropy" unless otherwise noted. In the present paper, we consider the entanglement entropy only for the one-body density matrix of fermion systems. The entanglement entropy that is defined by the one-body density matrix is given as

$$S = -\mathrm{Tr}\rho \log \rho = -\sum_l \rho_l \log \rho_l. \tag{8}$$

The entanglement entropy is zero if a wave function $|\Psi^{(A)}\rangle$ is a Slater determinant, because $\rho_l = 1$ for occupied single-particle states and $\rho_l = 0$ for unoccupied single-particle states. This means that a system has a non-zero positive value of the entanglement entropy only if the system contains many-body correlations beyond a Slater determinant, i.e., if the system is entangled.

2.2.2. *Schmidt number*

Another entanglement measure is the so-called Schmidt number, which was introduced by Grobe et al. and used to measure many-body correlations in atomic and nuclear physics [13–15]. The Schmidt number K is defined as

$$K = \frac{A}{\sum_l \rho_l^2} = \frac{A}{\mathrm{Tr}\rho^2}, \tag{9}$$

which estimates the number of states involved in the Schmidt decomposition. K equals unity if a wave function $|\Psi^{(A)}\rangle$ is a Slater determinant, and K is greater than unity for entangled states. By analogy to the entanglement entropy, which is generated by the entanglement, it is useful to consider the quantity $K-1$,

$$K - 1 = \frac{A}{\sum_l \rho_1^2} - 1 = \frac{\sum_l \left(\rho_l - \rho_l^2\right)}{\sum_l \rho_l^2}. \tag{10}$$

It is clear that $K-1=0$ only for non-entangled states because $\rho_l^2 = \rho_l$, i.e., $\hat{\rho}_\Psi^2 = \hat{\rho}_\Psi$ is satisfied only if a state is given by a Slater determinant. This means that a non-zero positive value of $K-1$ is generated by entanglement, that is, many-body correlations beyond a Slater determinant. One of the merits of the K number is that it is given by $\mathrm{Tr}\rho^2$ which can be calculated by the matrix element ρ_{pq} in an arbitrary basis without the diagonalization of the one-body density matrix.

We should note that the logarithm of the Schmidt number is nothing but the Rényi entanglement entropy of order 2 (Rényi-2 entanglement entropy) for the one-body density matrix,

$$\log K = S_2^{\mathrm{Renyi}}, \tag{11}$$

$$S_\xi^{\mathrm{Renyi}} = \frac{1}{1-\xi} \log\left\{\frac{\mathrm{Tr}\rho^\xi}{A}\right\}. \tag{12}$$

It is known that, in the $\xi \to 1$ limit, the Rényi entanglement entropy becomes equal to the von Neumann entanglement entropy. In this paper, we discuss the Schmidt number instead of Rényi-2 entropy though they are equivalent entanglement measures.

2.2.3. *Extension of Schmidt number*

In the present paper, we propose an entanglement measure which is regarded as a generalized version of the Schmidt number. As shown in Eq. (10), the origin of non-zero contributions in $K-1$ is a partially occupied single-particle state with $0 < \rho_l < 1$. Ignoring the total scaling factor $1/\sum_l \rho_l^2$, the contribution $W(\rho_l)$ (the weight function) of a single-particle state with occupation probability $0 < \rho < 1$ in $K-1$ has the ρ_l dependence $W(\rho_l) = \rho_l - \rho_l^2$, which is different from the weight function $W(\rho_l) = -\rho_l \log \rho_l$ in the entanglement entropy S. The former has relatively small weights for single-particle states with small occupation probability $\rho_l < 1/2$ compared with the latter, although the occupied $\rho_l = 1$ and unoccupied $\rho_l = 0$ single-particle states have no weight in both cases (see the ρ dependence of the weight functions in Fig. 1). We introduce here an alternative weight function, $W(\rho_l) = \rho_l^\gamma(1-\rho_l)$, and define an entanglement measure K_γ by extending the entanglement measure K as follows:

$$K_\gamma = \frac{\sum_l \rho_l^\gamma}{\sum_l \rho_l^{(1+\gamma)}} = \frac{\mathrm{Tr}\rho^\gamma}{\mathrm{Tr}\rho^{(1+\gamma)}}, \tag{13}$$

$$K_\gamma - 1 = \frac{\sum_l \rho_l^\gamma(1-\rho_l)}{\sum_l \rho_l^{(1+\gamma)}}, \tag{14}$$

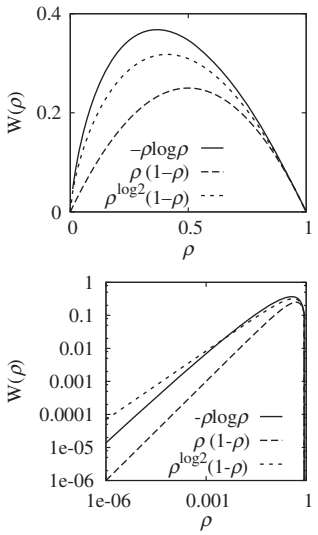

Fig. 1. Weight functions $W(\rho) = -\rho \log \rho$, $\rho(1-\rho)$, and $\rho^{\log 2}(1-\rho)$ for S, K, and $K_{\log 2}$, respectively.

where the parameter γ is a positive constant. In the case of $\gamma = 1$, the K_γ number becomes consistent with the Schmidt number K. Similarly to the known entanglement measures (S and $K-1$), $K_\gamma - 1$ equals zero only for a Slater determinant, whereas a non-zero positive value of $K_\gamma - 1$ is generated by entanglement, that is, many-body correlations beyond a Slater determinant. Note that the diagonalization of the density matrix is required to obtain the K_γ number for a non-integer γ differently from the K number. In this paper, we choose $\gamma = \log 2$ which gives the weight function $W(\rho_l) = \rho_l^{\log 2}(1-\rho_l)$ having ρ_l dependence similar to $W(\rho_l) = -\rho_l \log \rho_l$ for the entanglement entropy in $0.001 \lesssim \rho \leq 1$ (see Fig. 1).

It should be noted that $\log K_\gamma$ is given by the Rényi entanglement entropy of order γ and $1+\gamma$ as

$$\log K_\gamma = (1-\gamma) S_\gamma^{\text{Renyi}} + \gamma S_{1+\gamma}^{\text{Renyi}}. \tag{15}$$

2.3. *Spatial distributions of entanglement measures*

To investigate the spatial distribution of the "important single-particle states" that contribute to the non-zero entanglement entropy, we have defined the spatial distribution $s(\boldsymbol{r})$ of the entanglement entropy, as introduced in the previous paper [25], as

$$S = \sum_l (-\rho_l \log \rho_l) = \int s(\boldsymbol{r}) d\boldsymbol{r}, \tag{16}$$

$$s(\boldsymbol{r}) = \sum_l (-\rho_l \log \rho_l)\, \phi_l^*(\boldsymbol{r}) \phi_l(\boldsymbol{r}). \tag{17}$$

Here the factor $-\rho_l \log \rho_l$ is the contribution of the single-particle state $\phi_l(\boldsymbol{r}) = \langle \boldsymbol{r}|l\rangle$ in S, and $\phi_l^*(\boldsymbol{r})\phi_l(\boldsymbol{r})$ means the density distribution in $|l\rangle$ and is normalized as $\int \phi_l^*(\boldsymbol{r})\phi_l(\boldsymbol{r}) d\boldsymbol{r} = 1$. Therefore, the distribution $s(\boldsymbol{r})$ reflects spatial distributions of the important single-particle states $|l\rangle$ that contribute to the total entanglement entropy, whereas it is hardly affected by almost-occupied single-particle states having $\rho_l \approx 1$. The expression of S with $s(\boldsymbol{r})$ is analogous to that of the particle number

with the density distribution,

$$A = \sum_l \rho_l = \int \rho(\boldsymbol{r}) d\boldsymbol{r}, \tag{18}$$

$$\rho(\boldsymbol{r}) = \sum_l \rho_l \phi_l^*(\boldsymbol{r}) \phi_l(\boldsymbol{r}). \tag{19}$$

Note that the distribution $s(\boldsymbol{r})$ is not determined only by local information at the position $\boldsymbol{r}$. It is different from the density distribution $\rho(\boldsymbol{r})$ which is determined only by the local information.

We also define the distributions $\kappa(\boldsymbol{r})$ and $\kappa_\gamma(\boldsymbol{r})$ for $K-1$ and $K_\gamma - 1$, to see spatial distributions of the single-particle states that gives significant contributions to total values of $K-1$ and $K_\gamma - 1$, respectively:

$$K - 1 = \frac{\sum_l \left(\rho_l - \rho_l^2\right)}{\sum_l \rho_l^2} = \int \kappa(\boldsymbol{r}) d\boldsymbol{r}, \tag{20}$$

$$\kappa(\boldsymbol{r}) = \sum_l \frac{1}{\sum_l' \rho_l'^2} \left(\rho_l - \rho_l^2\right) \phi_l^*(\boldsymbol{r}) \phi_l(\boldsymbol{r}) = \sum_l \frac{K}{A} \left(\rho_l - \rho_l^2\right) \phi_l^*(\boldsymbol{r}) \phi_l(\boldsymbol{r}), \tag{21}$$

and

$$K_\gamma - 1 = \frac{\sum_l \rho_l^\gamma (1-\rho_l)}{\sum_l \rho_l^{1+\gamma}} = \int \kappa_\gamma(\boldsymbol{r}) d\boldsymbol{r}, \tag{22}$$

$$\kappa_\gamma(\boldsymbol{r}) = \sum_l \frac{1}{\sum_{l'} \rho_{l'}^{1+\gamma}} \rho_l^\gamma (1-\rho_l) \phi_l^*(\boldsymbol{r}) \phi_l(\boldsymbol{r}). \tag{23}$$

Similarly to $s(\boldsymbol{r})$, these distributions, $\kappa(\boldsymbol{r})$ and $\kappa_\gamma(\boldsymbol{r})$, show spatial distributions of the important single-particle states $|l\rangle$ that contribute to the total amount of $K-1$ and $K_\gamma - 1$, respectively. Note that these distributions are not local quantities.

3. S, K, and K_γ of ideal states in a toy model

In this section, we discuss behaviors of S, K, and K_γ for correlated (entangled) states composed of delocalized clusters in a toy model. Here, γ in the K_γ number is assumed to be $0 < \gamma < 1$.

Let us consider n_f species of particles. For instance, $n_f = 2$ for spin up and down fermions, and $n_f = 4$ for spin up and down protons and neutrons. We use the label σ for species of fermions such as $\sigma = p\uparrow, p\downarrow, n\uparrow, n\downarrow$ for nuclear systems. We consider an A-body system containing the same number $n = A/n_f$ of σ particles. We assume that the system is symmetric for the exchange of species, that is, single-particle orbitals are occupied by all species of particles with an equal weight. Then the density matrix is diagonal with respect to σ, and all species of particles have the same occupation probability $\rho_{\sigma l} = \rho_l$ independent of σ. We consider the one-body density matrix and operator in the reduced space with dimension n and define the entanglement measures, S, K, and K_γ, for a species of particles by using the reduced matrix of the one-body density. The total entanglement entropy $S_{\rm total}$ and the total numbers $K_{\rm total}$ and $K_{\gamma,{\rm total}}$ are given by the measures for each species as

$S_{\rm total} = n_f S$, $K_{\rm total} = K$, and $K_{\gamma,{\rm total}} = K_\gamma$. In this paper, we discuss S, K, and K_γ for a species of particles.

For simplicity, A particles are assumed to stay on sites in a space. The number of available sites (single-particle states) is m and we use the label k_j for the jth site. Let us first consider a system of $A = n_f$ particles. If an A-body state is an ideal state of independent particles, the wave function can be written by a simple product of single-particle wave functions,

$$\Psi(1, 2, \ldots, n_f) = \psi(1)\psi(2)\cdots\psi(n_f), \tag{24}$$

$$\psi(i) = \sum_{k=k_1,k_2,\ldots,k_m} c(k)\phi_k(i). \tag{25}$$

For instance, $c(k)$ is constant as $c(k) = 1/\sqrt{m}$ for a free gas state. For such a non-entangled state, $S = 0$, $K - 1 = 0$, and $K_\gamma - 1 = 0$ because the one-body density operator is given as $\hat{\rho}_\Psi = |\psi\rangle\langle\psi|$ and satisfies $\hat{\rho}_\Psi^2 = \hat{\rho}_\Psi$. Another example is a "localized cluster" system, where all particles are localized at one site k_j to form a composite particle (a cluster) at k_j. The wave function is given as

$$\Psi(1, 2, \ldots, n_f) = \prod_{i=1}^{n_f} \phi_{k_j}(i). \tag{26}$$

This wave function for a localized cluster also has zero measures, $S = 0$, $K - 1 = 0$, and $K_\gamma - 1 = 0$, because the one-body density operator is given as $\hat{\rho}_\Psi = |\phi_{k_j}\rangle\langle\phi_{k_j}|$ and again satisfies $\hat{\rho}_\Psi^2 = \hat{\rho}_\Psi$. In other words, the localized cluster wave function is a non-entangled state.

We consider a state of a delocalized cluster in a strong correlation limit,

$$\Psi(1, 2, \ldots, n_f) = \frac{1}{\sqrt{m}} \left\{ \prod_{i=1}^{n_f} \phi_{k_1}(i) + \prod_{i=1}^{n_f} \phi_{k_2}(i) + \cdots \prod_{i=1}^{n_f} \phi_{k_m}(i) \right\}, \tag{27}$$

where the composite particle composed of $A = n_f$ particles moves freely in the entire space with an equal probability $\frac{1}{m}$. This is a highly entangled (strongly correlated) state, where, if a particle is observed at a certain site, all other particles are always observed at the same site. This is a strong coupling limit and an example of a delocalized cluster. The one-body density operator,

$$\hat{\rho}_\Psi = \sum_{j=1}^{m} \frac{1}{m} |k_j\rangle\langle k_j|, \tag{28}$$

corresponds to the Schmidt decomposition with the common Schmidt coefficients $1/m$. We get $S = \log m$, $K = m$, and $K_\gamma = m$. In general, if eigenvalues of ρ_l are constant, $\rho_l = 1/m_V$ ($l = 1, \ldots, m_V$) for a given number (m_V) of states and $\rho_l = 0$ for $l > m_V$, we get

$$S = \log m_V, \quad e^S = m_V, \tag{29}$$

$$K = m_V, \tag{30}$$

$$K_\gamma = m_V. \tag{31}$$

It indicates that e^S, K, and K_γ equal the number m_V of states involved in the Schmidt decomposition. m_V is regarded as the effective volume size. Note that, for a Slater determinant, e^S, K, and K_γ equal 1, indicating that the effective volume size is one which cannot be decomposed.

Next we consider an A-particle system of $n = A/n_f$ clusters. Here, n is the number of clusters (composite particles) formed by n_f constituent fermions. For a state of n localized clusters at n sites

$k = k_{j_1}, \ldots, k_{j_n}$, the wave function is given as

$$\Psi(1, 2, \ldots, A) = (n!)^{-n_f/2}\mathcal{A}\left\{\prod_{h=0}^{n-1}\phi_{k_{j_1}}(hn_f + 1)\cdots\phi_{k_{j_1}}(hn_f + n_f)\right\}$$
$$= (n!)^{-n_f/2}\mathcal{A}\left\{\phi_{k_{j_h}}(1)\cdots\phi_{k_{j_1}}(n_f)\cdot\cdots\cdot\phi_{k_{j_n}}(A - n_f + 1)\cdots\phi_{k_{j_n}}(A)\right\}. \quad (32)$$

Since the occupation probability is $\rho_l = 1$ for occupied single-particle states $k_{j_1}, \ldots, k_{j_n}$ and $\rho_l = 0$ for unoccupied single-particle states, the system has the zero value of the measures, $S = 0$, $K - 1 = 0$, and $K_\gamma - 1 = 0$.

Let us consider a state of n clusters in the delocalized limit where all clusters are delocalized and move freely in a volume size m_V like a gas. For this state of delocalized clusters, the occupation probability is $\rho_l = n/m_V$ for $l = 1, \ldots, m_V$. m_V should not be less than n because of the Pauli principle for n fermions. The measures of this delocalized cluster system are

$$S = n\log\frac{m_V}{n}, \quad e^{S/n} = \frac{m_V}{n}, \quad (33)$$
$$K = \frac{m_V}{n}, \quad (34)$$
$$K_\gamma = \frac{m_V}{n}. \quad (35)$$

This indicates that K and K_γ are consistent with $e^{S/n}$. $ne^{S/n}$, nK, and nK_γ equal the number m_V of the states involved in the Schmidt decomposition and they estimate the effective volume size of the delocalization of clusters. For the case of $m_V = n = A/n_f$, all m_V single-particle states are completely occupied by A particles and clusters cannot move at all. The state is equivalent to the localized cluster, and it has zero value, $S = 0$, $K - 1 = 0$, and $K_\gamma - 1 = 0$, of the entanglement measures. In the case where m_V is larger than n, the measures S, $K - 1$, and $K_\gamma - 1$ become positive, indicating that delocalization of clusters occurs and the system becomes an entangled state. In the case that m_V is much larger than n, the system corresponds to a low-density cluster gas and it is a highly entangled state.

Finally, we consider the case of a partial delocalization where $n - 1$ clusters are localized to form a core and only the last cluster is delocalized. This situation corresponds to an α cluster moving almost freely around a core nucleus. In this partially localized case of a delocalized cluster around a core, the occupation probability is $\rho_l = n/m_V$ for $l = 1, \ldots, m_V$ and $\rho_l = 1$ for the $n - 1$ single-particle states occupied by constituent particles of the core. Then, the measures of this partially delocalized system are

$$S = \log m_V, \quad e^{S/n} = m_V^{1/n}, \quad (36)$$
$$K = \frac{nm_V}{(n-1)m_V + 1}, \quad (37)$$
$$K_\gamma = \frac{(n-1)m_V^\gamma + m_V}{(n-1)m_V^\gamma + 1}. \quad (38)$$

In the low-density limit of large m_V, we get

$$K \to \frac{n}{n-1}, \quad (39)$$
$$K_\gamma \to m_V^{1-\gamma}. \quad (40)$$

Let us compare the fully delocalized cluster state and the partially delocalized cluster state in the large m_V limit (the large volume size limit). The former state corresponds to a dilute cluster gas, where all clusters are delocalized, moving freely like a gas, and is a highly entangled state. For the fully delocalized cluster state, all the entanglement measures are sensitive to m_V as given in Eqs. (33), (34), and (35). That is, $e^{S/n}$, K, and K_γ are equal to m_V/n and equivalently good indicators to measure the delocalization of clusters. However, for the latter case of the partial delocalization, which corresponds to a delocalized cluster around a core, $e^{S/n}$, K, and K_γ are not equivalent but show different dependencies on m_V. As clearly shown in Eqs. (36), (39), and (40), $e^{S/n}$ and K_γ increase as m_V increases, but K becomes constant and does not depend on m_V in the large m_V limit. This indicates that S and K_γ can be useful measures sensitive to partial delocalization in a subsystem, but K is insensitive to partial delocalization. The reason for the insensitivity of K is the significant contribution from fully occupied single-particle states with $\rho_l = 1$ in the denominator of the definition of the K number, which makes the contribution from the delocalized part minor. From another point of view, it is found that K can be a good probe to clarify whether delocalization of clusters occurs in the entire system or not. The m_V dependencies of $e^{S/n}$ and K_γ are powers of $1/n$ and $1-\gamma$, respectively. More generally, for the partially delocalized system that is composed of n_g delocalized clusters and n_0 localized clusters, the m_V dependencies of $e^{S/n}$ and K_γ in the large m_V limit are powers of n_g/n and $1-\gamma$, respectively. Here, n_g and n_0 are the numbers of delocalized and localized clusters, respectively, and $n_0 + n_g = n$. This means that, in the case $n_g/n > 1-\gamma$ of a small fraction of delocalized clusters, K_γ is more sensitive to the delocalization of clusters than $e^{S/n}$, whereas, in the case of $n_g/n \approx 1-\gamma$, the K_γ number has the m_V dependence similar to $e^{S/n}$.

4. Application to 1D nuclear systems of α clusters

In the present paper, we use the delocalized cluster wave functions in 1D for the linear-chain $n\alpha$ states which were investigated in the previous paper [25]. We also adopt the $\alpha + (2\alpha)$ wave functions for the state of an α cluster around a 2α core. We analyze the entanglement measures, S, K, and $K_{\log 2}$, and also their spatial distributions, and discuss the system size dependence of these measures.

4.1. Localized and delocalized α cluster wave functions in 1D

We briefly explain here the adopted model wave functions for (de)localized cluster states in 1D. More details of the model wave functions are described in the previous paper [25]. We consider intrinsic wave functions of the linear-chain $n\alpha$-cluster states aligned to the x axis. This means that the (de)localization of α clusters is defined for α-cluster motion along the x axis.

For a localized $n\alpha$-cluster wave function, we use the BB wave function [27]:

$$\Phi^{n\alpha}_{\rm BB}(\boldsymbol{R}_1, \ldots, \boldsymbol{R}_n) = \frac{1}{\sqrt{A!}}\mathcal{A}\left[\psi^\alpha_{\boldsymbol{R}_1} \cdots \psi^\alpha_{\boldsymbol{R}_n}\right], \tag{41}$$

$$\psi^\alpha_{\boldsymbol{R}_i} = \phi^{0s}_{\boldsymbol{R}_i}\chi_{p\uparrow}\phi^{0s}_{\boldsymbol{R}_i}\chi_{p\downarrow}\phi^{0s}_{\boldsymbol{R}_i}\chi_{n\uparrow}\phi^{0s}_{\boldsymbol{R}_i}\chi_{n\downarrow}, \tag{42}$$

$$\phi^{0s} = \left(\pi b^2\right)^{-3/4}\exp\left[-\frac{1}{2b^2}(\boldsymbol{r}-\boldsymbol{R}_i)^2\right]. \tag{43}$$

$\psi^\alpha_{\boldsymbol{R}_i}$ is the four-nucleon wave function of the ith α cluster expressed by the $(0s)^4$ harmonic oscillator (ho) shell-model configuration localized around the spatial position $\boldsymbol{R}_i$. χ is the spin–isospin part and ϕ^{0s} is the spatial part of the single-particle wave function. For 1D cluster states, the position parameter $\boldsymbol{R}_i$ is set to be $\boldsymbol{R}_i = (R_i, 0, 0)$, and the 1D BB wave function is expressed as $\Phi^{n\alpha}_{\rm BB}(R_1, \ldots, R_n)$. The parameter b for the α-cluster size is chosen to be $b = 1.376$ fm, as in Ref. [8]. Note that a

single BB wave function is a localized cluster wave function written by a Slater determinant of single-particle wave functions and it has exactly zero values of the measures, $S = 0$, $K - 1 = 0$, and $K_\gamma - 1 = 0$. General wave functions for 1D $n\alpha$ systems can be written by linear combination of BB wave functions $\Phi^{n\alpha}_{\rm BB}(R_1, \ldots, R_n)$.

For a delocalized cluster wave function, we use the 1D-THSR wave functions of $n\alpha$, which were proposed by Suhara et al. to describe the linear-chain 3α- and 4α-cluster states in ^{12}C and ^{16}O systems [8]. The 1D-THSR wave functions are given by linear combination of BB wave functions with a Gaussian weight:

$$\Phi^{n\alpha}_{\rm 1D-THSR}(\beta) = \int dR_1 \cdots dR_n \exp\left\{-\sum_{i=1}^{n}\frac{R_i^2}{\beta^2}\right\}\Phi^{n\alpha}_{\rm BB}(R_1, \ldots, R_n)$$
$$\propto \mathcal{A}\left[\prod_{i=1}^{n}\exp\left\{-\frac{2X_{ix}^2}{b^2} - \frac{2X_{iy}^2}{b^2} - \frac{X_{iz}^2}{\beta^2 + b^2/2}\right\}\phi(\alpha_i)\right], \tag{44}$$

where $\boldsymbol{X}_i$ is the center of mass (c.m.) coordinate of the ith α cluster and $\phi(\alpha_i)$ is the intrinsic wave function of the α cluster. If antisymmetrization is ignored, $\Phi^{n\alpha}_{\rm 1D-THSR}(\beta)$ expresses the $n\alpha$ state where all α clusters are confined in the y and z directions while they move in the x direction in the Gaussian orbit with the range parameter β. β corresponds to the system size of the 1D $n\alpha$ state. In the case where the system size β is as small as or smaller than the α-cluster size b, the 1D-THSR wave function is approximately equivalent to a localized cluster wave function given by a Slater determinant because of the antisymmetrization effect. As β increases, delocalization of α clusters occurs. When β is large enough compared with the α-cluster size b, the system goes to a dilute 1D α-cluster gas where n α clusters move almost freely like a gas in the x direction.

In the practical calculation, the R_i integration is approximated by summation on mesh points at 1 fm intervals in a finite box $|R_i| \leq 12$ fm:

$$\Phi^{n\alpha}_{\rm 1D-THSR}(\beta) \to \sum_{R_1=0,\pm1,\ldots,12} \cdots \sum_{R_n=0,\pm1,\ldots,12} \exp\left\{-\sum_{i=1}^{n}\frac{R_i^2}{\beta^2}\right\}\Phi^{n\alpha}_{\rm BB}(R_1, \ldots, R_n). \tag{45}$$

We have checked that the interval of the summation is small enough to give the converged result. For 2α, 3α, and 4α systems, we make a correction of the total c.m.m. to eliminate a possible artifact from β dependence in the total c.m.m., as in the previous paper, by shifting the cluster position, $R_i \to R'_i = R_i - R_G$, of basis BB wave functions ($\Phi^{n\alpha}_{\rm BB}$) in $\Phi^{n\alpha}_{\rm 1D-THSR}(\beta)$ with $R_G \equiv (R_1 + \cdots + R_n)/n$ as

$$\Phi^{n\alpha}_{\rm 1D-THSR}(\beta) \to \sum_{R_1=0,\pm1,\ldots} \cdots \sum_{R_n=0,\pm1,\ldots} \exp\left\{-\sum_{i=1}^{n}\frac{R_i^2}{\beta^2}\right\}\Phi^{n\alpha}_{\rm BB}\left(R'_1, \ldots, R'_n\right), \tag{46}$$

where the mesh points of the summation are truncated in a finite box $|R'_i| \leq 12$ fm. The correction of c.m.m. is equivalent to replacing the β-dependent c.m.m. $\Phi_G(\beta)$ in the original 1D-THSR with $\Phi_G(0)$ localized at the origin to eliminate the β dependence in the c.m.m.,

$$\Phi^{n\alpha}_{\rm 1D-THSR} = \Phi_G(\beta)\Phi_{\rm int}(\beta) \to \Phi_G(0)\Phi_{\rm int}(\beta), \tag{47}$$

$$\Phi_G(\beta) \propto \exp\left\{-\frac{A}{2b^2}X_{Gx}^2 - \frac{A}{2b^2}X_{Gy}^2 - \frac{A}{4\beta^2 + 2b^2}X_{Gz}^2\right\}, \tag{48}$$

where $\boldsymbol{X}_G$ is the total c.m. coordinate and $\Phi_{\rm int}(\beta)$ is the intrinsic wave function which is independent of $\boldsymbol{X}_G$. The 1D-THSR wave function of 1α without the c.m.m. correction expresses a system of an α cluster bound in an external field, which is not a realistic state for an isolated nucleus, whereas those of 2α, 3α, and 4α with the c.m.m. correction correspond to self-bound $n\alpha$ systems with linear-chain structures predicted in nuclear states such as excited states of ^{12}C and ^{16}O. In this paper, we discuss the entanglement measures for 1α with no c.m.m. correction (nc) and those for 2α, 3α, and 4α with the c.m.m. correlation. We also show the entanglement entropy for 2α with no c.m.m. correction, just for comparison.

We also use the 1D-THSR wave function of $\alpha + (2\alpha)$ for the case of an α cluster around the 2α core,

$$\Phi^{\alpha-(2\alpha)}_{\rm 1D-THSR}(\beta) = \int dR_1 \exp\left\{-\frac{R_1^2}{\beta^2}\right\} \Phi^{3\alpha}_{\rm BB}(R_1, R_2 = +\varepsilon, R_3 = -\varepsilon), \tag{49}$$

where the 2α core is located at the origin and an α cluster is distributed around the core with a Gaussian weight. When β is large enough compared with the α-cluster size b, the wave function describes a delocalized α cluster around the 2α core at the origin. This wave function is associated with the partially delocalized cluster wave function in the toy model discussed previously. We use a small value of $\varepsilon = 0.02$ fm to describe the 2α core almost equivalent to the h.o. $(0s)^4(0p_x)^4$ configuration. This wave function was originally introduced in the previous paper to describe the $\alpha+^{16}$O cluster states in ^{20}Ne.

4.2. *Calculation of density matrix for linear nα states*

We calculate the matrix elements of the one-body density operator for linear-chain α-cluster states by the expansion of localized Gaussian bases,

$$\phi^{0s}_{X_k} = (\pi b^2)^{-3/4} \exp\left[-\frac{1}{2b^2}(\boldsymbol{r} - \boldsymbol{X}_k)^2\right], \tag{50}$$

with $\boldsymbol{X}_k = (0, 0, X_k)$. We construct an orthonormal basis set $\{\phi_p(\boldsymbol{r})\}$ from the bases $\{\phi^{0s}_{X_k}(\boldsymbol{r})\}$ $(k = 1, \ldots, 35)$ with $X_k = 0.75j$ fm $(j = 0, \pm1, \ldots, 15)$. For the single-particle bases $\{\phi_p(\boldsymbol{r})\}$, we calculate the one-body density matrix ρ_{pq}:

$$\begin{aligned}\rho_{pq} &= \left\langle \Psi^{(A)} | c_q^\dagger c_p | \Psi^{(A)} \right\rangle, \\ &= \int d\boldsymbol{r} d\boldsymbol{r}' \phi_p^*(\boldsymbol{r}) \rho^{(1)}(\boldsymbol{r}; \boldsymbol{r}') \phi_q(\boldsymbol{r}'), \end{aligned} \tag{51}$$

$$\rho(\boldsymbol{r}; \boldsymbol{r}') = \left\langle \Psi^{(A)} | a^\dagger(\boldsymbol{r}'\sigma) a(\boldsymbol{r}\sigma) | \Psi^{(A)} \right\rangle. \tag{52}$$

Note that, for a given wave function $\Psi^{(A)}$ of an $n\alpha$ state that is expressed by a linear combination of BB wave functions $\Phi^{n\alpha}_{\rm BB}(R_1, \ldots, R_n)$, and also for the 1D-THSR wave function described by a linear combination of a finite number of BB wave functions in the present calculation, $\rho(\boldsymbol{r}; \boldsymbol{r}')$ can be expressed by a linear combination of $\phi^{0s}_{R_i}(\boldsymbol{r})$ and $\phi^{0s}_{R_i}(\boldsymbol{r}')$, and hence the matrix elements ρ_{pq} can be practically calculated. Finally, by diagonalizing ρ_{pq}, we obtain the eigenvalues ρ_l and the single-particle bases $\phi_l(\boldsymbol{r}) = \langle \boldsymbol{r}|l\rangle$ of the one-body density matrix by the unitary transformation of $\{\phi_p(\boldsymbol{r})\}$.

With the obtained eigenvalues ρ_l and the single-particle bases $\phi_l(\boldsymbol{r})$ of the one-body density matrix, we calculate the measures (S, K, and $K_{\log 2}$) and spatial distributions ($s(\boldsymbol{r})$, $\kappa(\boldsymbol{r})$, and $\kappa_\gamma(\boldsymbol{r})$). More details of the practical calculation are described in the previous paper [25]. the spatial distributions

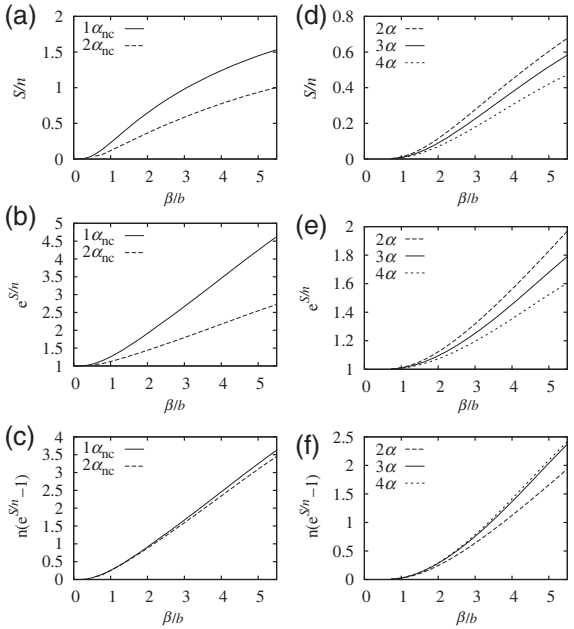

Fig. 2. System size β/b dependence of the entanglement entropy S and $e^{S/n}$ in the 1D-THSR wave functions of $n\alpha$. $n(e^{S/n}-1)$ is also shown. The 1D-THSR wave functions with the total c.m.m. correction are used for 2α, 3α, and 4α systems, and that with no c.m.m. correction is used for the 1α system ($1\alpha_{\rm nc}$). The results of the 1D-THSR wave function with no c.m.m. correction for the 2α system ($2\alpha_{\rm nc}$) are also shown for comparison.

$s(\boldsymbol{r})$, $\kappa(\boldsymbol{r})$, and $\kappa_\gamma(\boldsymbol{r})$ and the density distribution $\rho(\boldsymbol{r})$ are integrated out along the y and z axes, and we get the distributions $s(x)$, $\kappa(x)$, $\kappa_\gamma(x)$, and $\rho(x)$, projected onto the x axis.

4.3. $n\alpha$ cluster states

We analyze S, K, and $K_{\log 2}$ of the 1D $n\alpha$ states written by the 1D-THSR wave functions, $\Phi^{n\alpha}_{\rm 1D-THSR}(\beta)$. Figure 2 shows the system size dependence of the entanglement entropy of the 1α state with no c.m.m. correction ($1\alpha_{\rm nc}$), and 2α, 3α, and 4α states with the c.m.m. correction, as well as that of a 2α state with no c.m.m. correction ($2\alpha_{\rm nc}$), S/n, $e^{S/n}$, and $n(e^{S/n}-1)$ are plotted as functions of the dimensionless system size β/b. In the $\beta/b=0$ limit, the entanglement entropy equals zero, because the 1D-THSR wave functions are equivalent to localized $n\alpha$ cluster wave functions in this limit. As β/b increases, delocalization of clusters occurs and the entanglement entropy is generated. $e^{S/n}$ for the $1\alpha_{\rm nc}$ state increases almost linearly to β/b as expected from a naive picture that a cluster moves freely in a finite volume, which is decomposed into $m_V \sim \beta/b$ states by the quantum decoherence in the one-body density matrix. Similarly to the $1\alpha_{\rm nc}$ state, S for 2α, 3α, and 4α states increases with the increase of the system size, indicating that the entanglement entropy is generated as the delocalization of clusters is enhanced. $e^{S/n}$ for 2α, 3α, and 4α states also shows almost linear dependence on β/b. The $n(e^{S/n}-1)$ plots in Figs. 2(c) and 2(d) show a good correspondence of the β dependence of the entanglement entropy between $1\alpha_{\rm nc}$ and $2\alpha_{\rm nc}$, and that between 2α, 3α, and 4α states. The values of $n(e^{S/n}-1)$ for 2α, 3α, and 4α are relatively smaller compared with those for $1\alpha_{\rm nc}$ and $2\alpha_{\rm nc}$ because of the c.m.m. correction performed for the 2α, 3α, and 4α states.

Let us compare the other measures, K and $K_{\log 2}$, with the entanglement entropy. Figure 3 shows the system size dependence of $e^{S/n}$, K, and $K_{\log 2}$ of $1\alpha_{\rm nc}$, 2α, 3α, and 4α states. K and $K_{\log 2}$ show β/b dependence quite similar to that of $e^{S/n}$ except for global normalization factors. This result

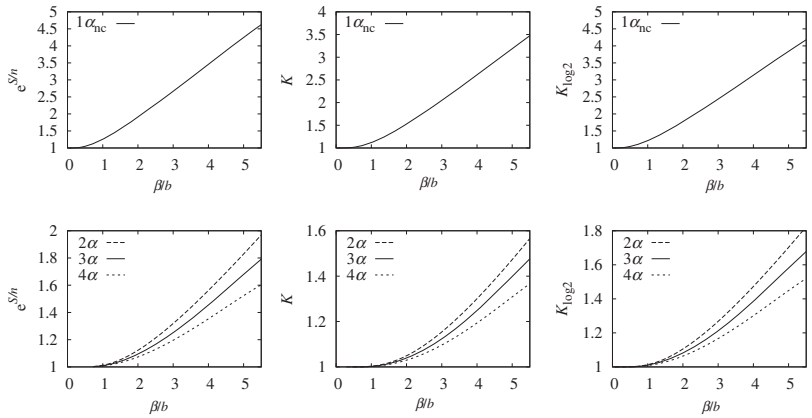

Fig. 3. Comparison of system size β/b dependencies between $e^{S/n}$, K, and $K_{\log 2}$ in the 1D-THSR wave functions of $n\alpha$.

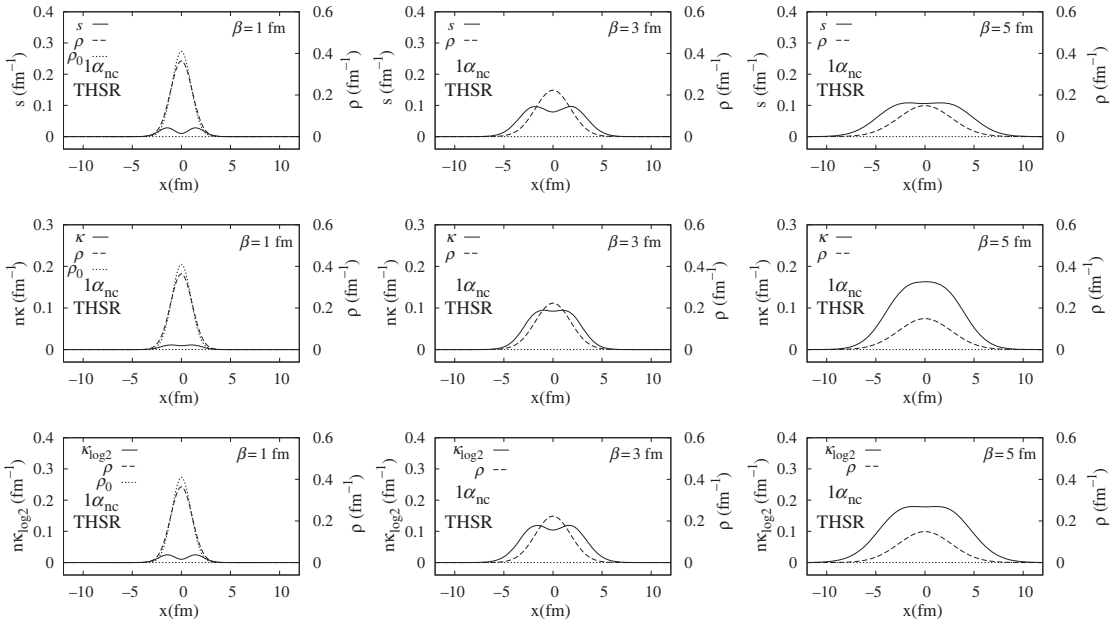

Fig. 4. Spatial distributions $s(x)$, $\kappa(x)$, and $\kappa_{\log 2}(x)$ of S, $K-1$, and $K_{\log 2}-1$ in the 1D-THSR wave functions of $1\alpha_{\rm nc}$ with $\beta = 1$ fm, 3 fm, and 5 fm. The corresponding dimensionless system sizes are $\beta/b = 0.73$, 2.18, and 3.63. The density distribution $\rho(x)$ is also shown.

indicates that the entanglement entropy, K, and $K_{\log 2}$ can be approximately equivalent measures for the cluster delocalization of $n\alpha$ states. This is consistent with the naive expectation from the analysis of the delocalized cluster states in the toy model discussed in the previous section. It means that $ne^{S/n}$, nK, and $nK_{\log 2}$ estimate the number of states involved in the Schmidt decomposition as shown in Eqs. (33), (34), and (35).

We also compare the spatial distributions of these measures, $s(x)$, $\kappa(x)$, and $\kappa_{\log 2}(x)$, of $1\alpha_{\rm nc}$ in Fig. 4. The density distribution is also shown. As described previously, $s(x)$, $\kappa(x)$, and $\kappa_{\log 2}(x)$ reflect spatial distributions of the important single-particle states that give non-zero contributions to the total measures S, $K-1$, $K_{\log 2}-1$, respectively. Note that the shape, in particular the spatial broadness, of the distributions is of importance, but their global scaling (normalization) is not so meaningful. It is found that $s(x)$ and $\kappa_{\log 2}(x)$ show quite similar distributions to each other. They are

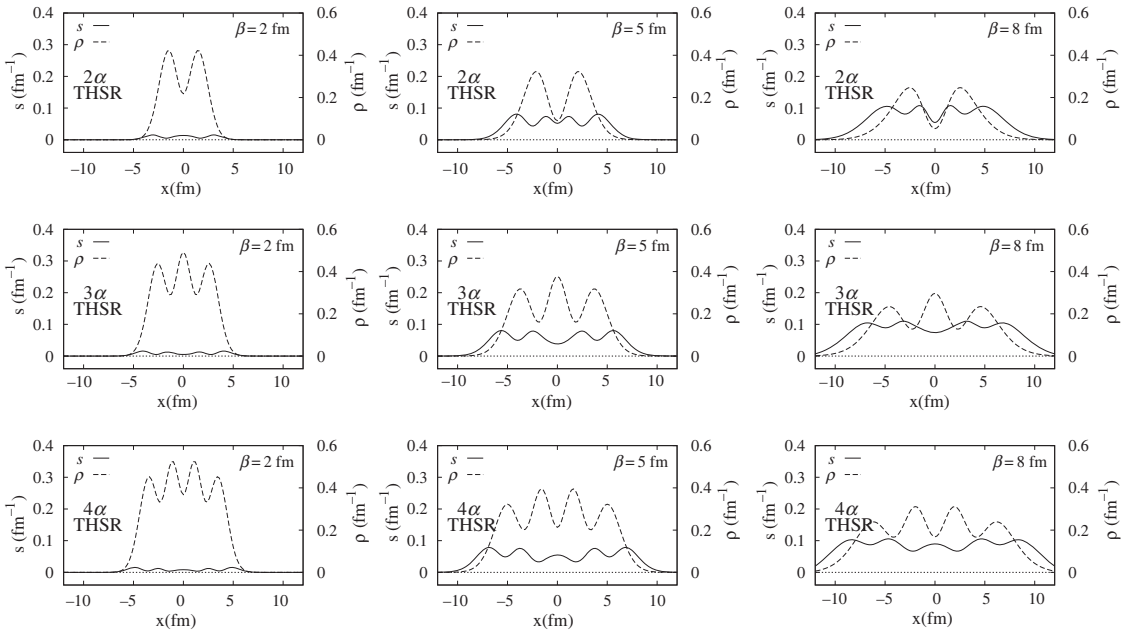

Fig. 5. Spatial distribution, $s(x)$, of the entanglement entropy S in the 1D-THSR wave functions of 2α, 3α, and 4α with $\beta = 2$ fm, 5 fm, and 8 fm. The corresponding dimensionless system sizes are $\beta/b = 1.45$, 3.63, and 5.81. The density distribution $\rho(x)$ is also shown.

more broadly distributed than the density distribution, indicating that S and $K_{\log 2} - 1$ are generated in low-density regions but relatively suppressed in high-density regions. Differently from $s(x)$ and $\kappa_{\log 2}(x)$, the enhancement in low-density regions and the suppression in high-density regions are relatively weak in $\kappa(x)$. As a result, the spatial extent of $\kappa(x)$ is not as remarkable as that of $s(x)$ and $\kappa_{\log 2}(x)$. This difference in the spatial distributions of S, $K - 1$, $K_{\log 2} - 1$ comes from the different weight functions $W(\rho)$, namely, S and $K_{\log 2} - 1$ are relatively sensitive to single-particle states with low occupation probability compared with $K - 1$, as already shown in Fig. 1. The distributions $s(x)$, $\kappa(x)$, and $\kappa_{\log 2}(x)$ for the 2α, 3α, and 4α states are shown in Figs. 5–7 along with the density distribution. Similarly to the $1\alpha_{\rm nc}$ state, $s(x)$ and $\kappa_{\log 2}(x)$ are more broadly distributed than the density distribution and also slightly broader than $\kappa(x)$, indicating again that S and $K_{\log 2} - 1$ are generated in low-density regions but suppressed in high-density regions.

In the present result, we find that S, K, and $K_{\log 2}$ can be useful measures to estimate the entanglement caused by the delocalization of clusters in the 1D $n\alpha$ states given by the 1D-THSR wave functions. As the system size increases, delocalization of clusters develops and non-zero S, $K - 1$, and $K_{\log 2} - 1$ are generated. In the spatial distributions of these entanglement measures, significant contributions come from low-density regions rather than high-density regions. Quantitatively, the Schmidt number (K) is less sensitive to low-occupation-probability single-particle states than the entanglement entropy (S) and the $K_{\log 2}$ number resulting in the less-broad distribution of $\kappa(x)$ than $s(x)$ and $\kappa_{\log 2}(x)$, which are notably broader than the density distribution.

4.4. An α cluster around a 2α core

We investigate S, K, and $K_{\log 2}$ of $\alpha + (2\alpha)$ cluster wave functions. We use the 1D-THSR wave function $\Phi^{\alpha-(2\alpha)}_{\rm 1D-THSR}(\beta)$ in Eq. (49) for the $\alpha + (2\alpha)$ states associated with the partially delocalized cluster wave function. We also adopt the parity-projected BB wave function with the fixed α–(2α)

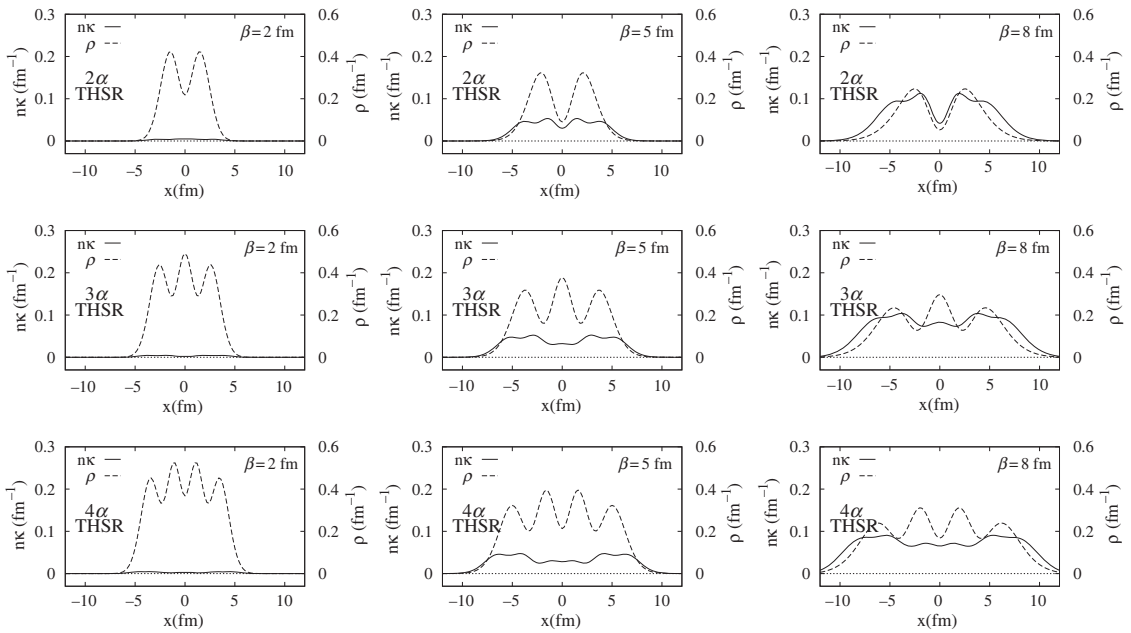

Fig. 6. As Fig. 5, but spatial distribution $\kappa(x)$ for $K-1$.

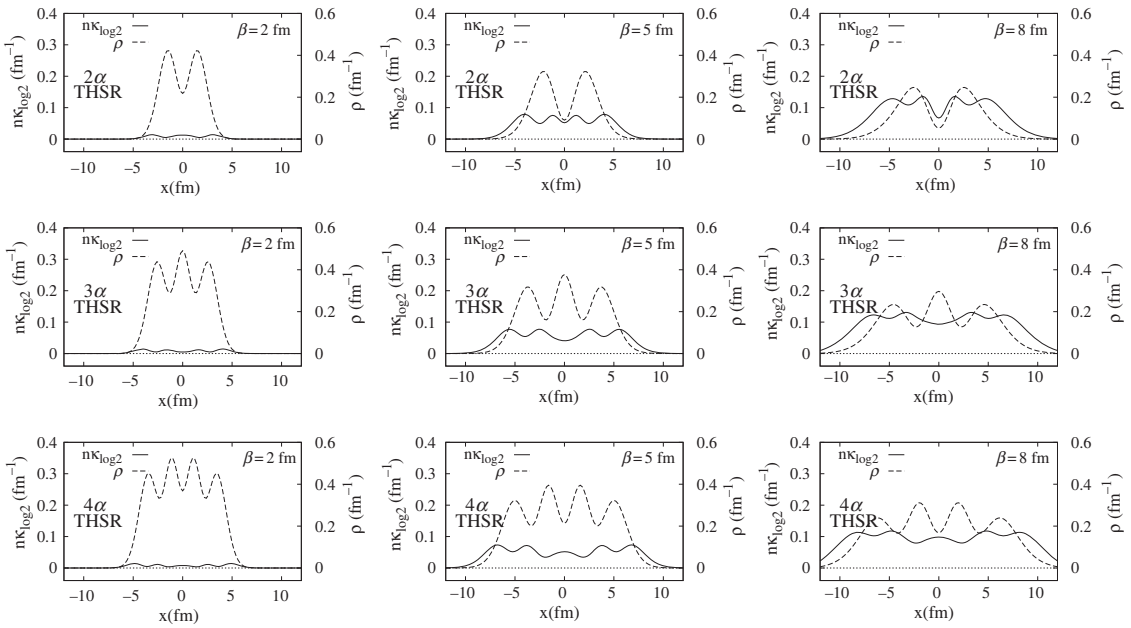

Fig. 7. As Fig. 5, but spatial distribution $\kappa_{\log 2}(x)$ for $K_{\log 2}-1$.

distance d as used in the previous paper:

$$\Phi_{\rm BB}^{\alpha-(2\alpha),+}(d) = (1+\hat{P}_r)\Phi_{\rm BB}^{3\alpha}(R_1=d, R_2=+\varepsilon, R_3=-\varepsilon)$$
$$= \Phi_{\rm BB}^{3\alpha}(R_1=d, R_2=+\varepsilon, R_3=-\varepsilon)$$
$$+ \Phi_{\rm BB}^{3\alpha}(R_1=-d, R_2=+\varepsilon, R_3=-\varepsilon), \quad (53)$$

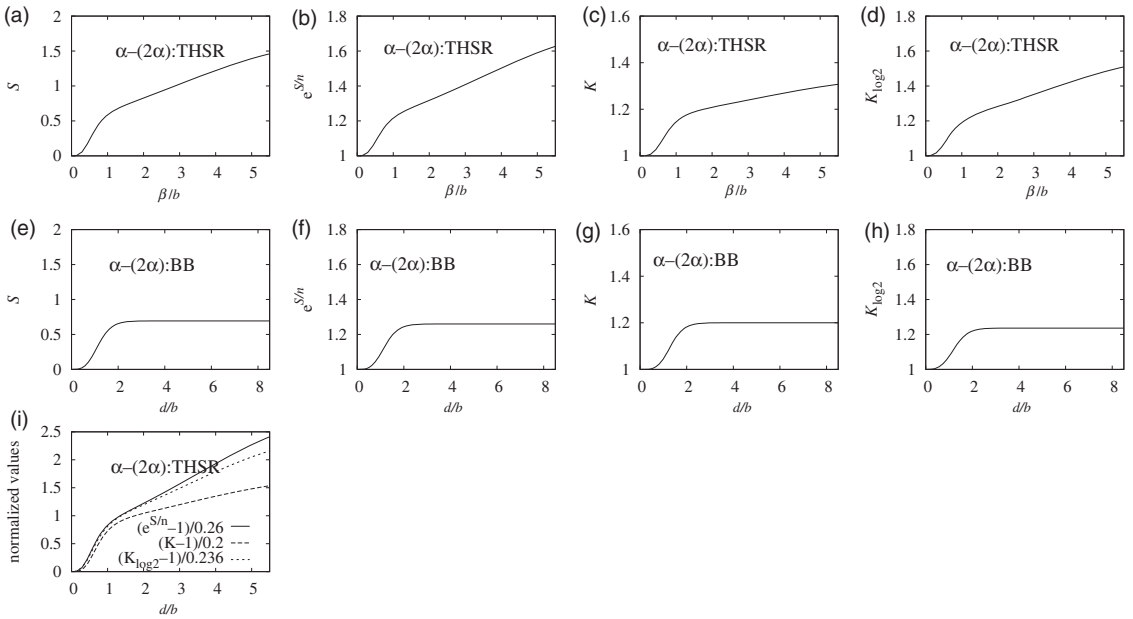

Fig. 8. (a)–(d) System size β/b dependence of S, $e^{S/n}$, K, and $K_{\log 2}$ in the 1D-THSR wave function of $\alpha + (2\alpha)$, and (e)–(h) d/b dependence of S, $e^{S/n}$, K, and $K_{\log 2}$ in the parity-projected BB wave function of $\alpha + (2\alpha)$. (i) Scaled measures $(e^{S/n} - 1)/0.26$, $(K - 1)/0.2$, $K_{\log 2}/0.236$ in the 1D-THSR wave function of $\alpha + (2\alpha)$, normalized to the large-d limit values of the parity-projected BB wave function.

where $\hat{P}_r$ is the parity transformation operator. Note that $\Phi_{\rm BB}^{\alpha-(2\alpha),+}(d)$ is given by the linear combination of two Slater determinants. This corresponds to the symmetry-restored state where the parity symmetry is broken in the intrinsic state because of the cluster development.

Figure 8 shows S, K, and $K_{\log 2}$ as well as $e^{S/n}$ for the 1D-THSR wave function and the parity-projected BB wave function of the $\alpha + (2\alpha)$ system. Looking at the result of the parity-projected BB wave function, we find that, as d increases and the parity symmetry is broken in the intrinsic wave function, non-zero values of S, $K - 1$, and $K_{\log 2}$ are generated in the projected state even though the intrinsic wave function before the parity projection is the localized cluster wave function. When d is large enough, $\hat{P}_r \Phi_{\rm BB}^{3\alpha}$ becomes independent of $\Phi_{\rm BB}^{3\alpha}$, and we get $S \to \log 2 = 0.693$, $K - 1 \to 1/5 = 0.2$, $K_{\log 2} - 1 \to 0.236$ from the eigenvalues of the one-body density matrix, $\rho_1 = \rho_2 = 1$ and $\rho_3 = \rho_4 = 1/2$. This means that non-zero values of S, $K - 1$, and $K_{\log 2} - 1$ are generated by the symmetry breaking and restoration. Let us turn to the result of the 1D-THSR wave function. In the $\beta/b = 0$ limit, S, $K - 1$, and $K_{\log 2} - 1$ are zero. In the $\beta/b \lesssim 1$ region, S, K, and $K_{\log 2}$ increase rapidly with the increase of β/b because of the symmetry breaking and restoration as seen in the parity-projected BB wave function. For $\beta/b \gtrsim 1$, S, K, and $K_{\log 2}$ increase gradually as the system size increases, indicating that delocalization of the cluster develops in this region.

As discussed in the previous section, the Schmidt number, K, should be less sensitive to the delocalization in the partially delocalized cluster states. To see the sensitivity of $e^{S/n}$, K, and $K_{\log 2}$ to the delocalization, we show in Fig. 8(i) the scaled measures $(e^{S/n} - 1)/0.26$, $(K - 1)/0.2$, and $K_{\log 2}/0.236$ in the 1D-THSR wave function of $\alpha + (2\alpha)$, normalized to the values of the large d limit of the parity-projected BB wave function. As expected from the analysis of the simple toy model, the result in Fig. 8(i) shows that K is not so sensitive to the delocalization of the cluster in the $\alpha + (2\alpha)$ state, whereas $e^{S/n}$ and $K_{\log 2}$ more strongly depend on the the system size in the $\beta/b \gtrsim 1$ region than K. The β/b dependence of $K_{\log 2}$ is quite similar to that of $e^{S/n}$, maybe because of the accidental

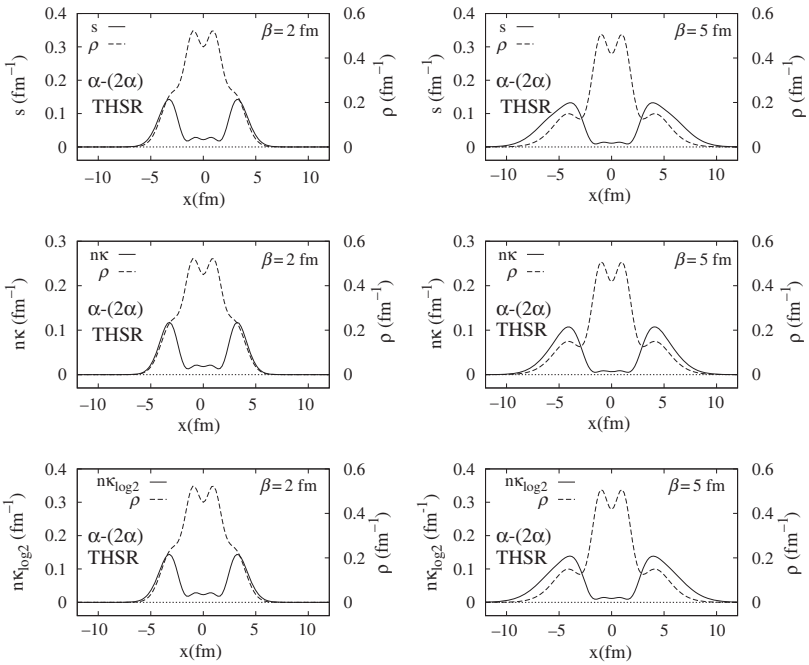

Fig. 9. Spatial distributions $s(x)$, $\kappa(x)$, and $\kappa_{\log 2}(x)$ of S, K, and $K_{\log 2}$ in the 1D-THSR wave functions of $\alpha + (2\alpha)$ with $\beta = 2$ fm and 5 fm. The corresponding dimensionless system sizes are $\beta/b = 1.45$ and 3.63. The density distribution $\rho(x)$ is also shown.

coincidence of the $m_V^{1/n}$ dependencies, $e^{S/n} \propto m_V^{1/n}$ and $K_\gamma \propto m_V^{(1-\gamma)}$, for the partially delocalized cluster state discussed in the simple toy model as $1/n = 1/3$ and $1 - \gamma = 1 - \log 2 = 0.31$.

Figure 9 shows the distributions $s(x)$, $\kappa(x)$, and $\kappa_{\log 2}(x)$ of S, $K - 1$, and $K_\gamma - 1$ as well as the density distribution in the 1D-THSR wave functions of $\alpha + (2\alpha)$ for $\beta = 2$ fm and 5 fm. It is clear that distributions $s(x)$, $\kappa(x)$, and $\kappa_{\log 2}(x)$ are strongly suppressed in the $|x| \lesssim 2$ fm range because of the Pauli blocking effect from the 2α core. In the $\beta = 5$ fm case delocalization occurs, and S and $K_\gamma - 1$ are generated in the low-density regions in particular at the long tail part. Similarly to the distributions in $n\alpha$ states, the distribution $\kappa(x)$ for $K - 1$ is not so enhanced in low-density regions as $s(x)$ and $\kappa_{\log 2}(x)$ because the Schmidt number K is relatively less sensitive to single-particle states with low occupation probability compared with the entanglement entropy and the $K_{\log 2}$ number.

5. Summary

We calculated the entanglement entropy (S) and the Schmidt number (K) defined by the one-body density matrix in the 1D α-cluster states to measure the entanglement caused by the delocalization of clusters in nuclear systems. We also proposed a new entanglement measure K_γ with a generalized form of the Schmidt number.

For the delocalized cluster states of $n\alpha$ given by the 1D-THSR wave functions, $e^{S/n}$, K, and $K_{\log 2}$ show good correspondence, indicating that the entanglement entropy, the Schmidt number, and the $K_{\log 2}$ number are almost equivalent entanglement measures to estimate the delocalization of a 1D gas of delocalized n α clusters. On the other hand, for the partially delocalized cluster state which contains a delocalized cluster and a core composed of localized clusters, the Schmidt number is not sensitive to the delocalization of the cluster around the core, whereas the entanglement entropy and the $K_{\log 2}$ number can be good indicators to measure the partial delocalization. In other words, the

Schmidt number can be a good probe to clarify whether the delocalization occurs for all clusters in the entire system or not, owing to the insensitivity to partial delocalization. We should comment that the Schmidt number corresponds to the the Rényi-2 entanglement entropy, $K = e^{S_2^{\rm Renyi}}$. This means that the equivalence in the fully delocalized cluster states and difference in the partially delocalized cluster states between $e^{S/n}$ and K are nothing but those between the von Neumann entanglement entropy and Rényi-2 entanglement entropy.

In the present analysis of 1D α-cluster states, the $K_{\log 2}$ number shows similar features to the entanglement entropy. It indicates that the $K_{\log 2}$ number can be an alternative measure to the entanglement entropy to estimate the delocalization in both cases of partially and fully delocalized cluster states. When the delocalized part is minor compared with the core part, the $K_{\log 2}$ number is more sensitive to the partial delocalization than the entanglement entropy, and hence is a promising measure.

We should point out that the calculation of the Schmidt number may be easier practically than those of the entanglement entropy and K_γ with a non-integer γ because the Schmidt number is given by $\mathrm{Tr}\rho^2$ for which the diagonalization of the one-body density matrix is not required. This could be an advantage of the Schmidt number in large-dimensional calculations because numerical errors might become a more serious problem in practical calculations of the entanglement entropy and the K_γ number.

Recently, comparison between von Neumann and Rényi-2 entanglement entropies have been discussed in various fields such as field theories [28]. The equivalence and difference between von Neumann and Rényi-2 entanglement entropies shown in the present study are general features and may be found in various quantum systems. The present study of entanglement measures in cluster wave functions of nuclear systems may shed light on the study of entanglement (correlation) in general quantum systems.

Acknowledgements

The author would like to thank H. Iida for helpful discussions. The calculations for this work have been done using computers at the Yukawa Institute for Theoretical Physics, Kyoto University. This work was supported by JSPS KAKENHI Grant No. 26400270.

References

[1] E. Uegaki, S. Okabe, Y. Abe, and H. Tanaka, Prog. Theor. Phys. **57**, 1262 (1977).
[2] A. Tohsaki, H. Horiuchi, P. Schuck, and G. Röpke, Phys. Rev. Lett. **87**, 192501 (2001).
[3] Y. Funaki, H. Horiuchi, A. Tohsaki, P. Schuck, and G. Röpke, Prog. Theor. Phys. **108**, 297 (2002).
[4] Y. Funaki, A. Tohsaki, H. Horiuchi, P. Schuck, and G. Ropke, Phys. Rev. C **67**, 051306 (2003).
[5] Y. Funaki, H. Horiuchi, W. von Oertzen, G. Röpke, P. Schuck, A. Tohsaki, and T. Yamada, Phys. Rev. C **80**, 064326 (2009).
[6] B. Zhou et al., Phys. Rev. C **86**, 014301 (2012).
[7] B. Zhou et al., Phys. Rev. Lett. **110**, 262501 (2013).
[8] T. Suhara, Y. Funaki, B. Zhou, H. Horiuchi, and A. Tohsaki, Phys. Rev. Lett. **112**, 062501 (2014).
[9] H. Morinaga, Phys. Rev. **101**, 254 (1956).
[10] Y. Kanada-En'yo, Prog. Theor. Exp. Phys. **2014**, 103D03 (2014).
[11] R. Grobe, K. Rzazewski, and J. H. Eberly, J. Phys. B **27**, L503 (1994).
[12] C. H. Bennett, H. J. Bernstein, S. Popescu, and B. Schumacher, Phys. Rev. A **53**, 2046 (1996).
[13] C. K. Law, Phys. Rev. A **71**, 034306 (2005).
[14] N. Sandulescu and G. F. Bertsch, Phys. Rev. C **78**, 064318 (2008).
[15] M. C. Tichy, F. Mintert, and A. Buchleitner, J. Phys. B **44**, 192001 (2011).
[16] P. Calabrese and J. L. Cardy, J. Stat. Mech. **0406**, P06002 (2004).
[17] M. B. Plenio, and S. Virmani, 2007, Quant. Inf. Comp. **7**, 1 (2007).
[18] L. Amico, R. Fazio, A. Osterloh, and V. Vedral, Rev. Mod. Phys. **80**, 517 (2008).

[19] R. Horodecki, P. Horodecki, M. Horodecki, and K. Horodecki, Rev. Mod. Phys. **81**, 865 (2009).
[20] T. Nishioka, S. Ryu, and T. Takayanagi, J. Phys. A **42**, 504008 (2009).
[21] J. Eisert, M. Cramer, and M. B. Plenio, Rev. Mod. Phys. **82**, 277 (2010).
[22] M. Dugić and J. Jeknić, Int. J. Theor. Phys. **45**, 2215 (2006).
[23] C. Chudzicki, O. Oke, and W. K. Wootters, Phys. Rev. Lett. **104**, 070402 (2010).
[24] A. M. Gavrilik and Yu. A. Mishchenko, Phys. Lett. A **376**, 1596 (2012).
[25] Y. Kanada-En'yo, Phys. Rev. C **91**, 034303 (2015).
[26] P. Ring and P. Schuck, *The Nuclear Many-Body Problem* Springer Verlag, New York, 1980.
[27] D. M. Brink, *International School of Physics "Enrico Fermi"* (Academic Press, New York and London, 1966), XXXVI, p. 247.
[28] P. Caputa, M. Nozaki, and T. Takayanagi, Prog. Theor. Exp. Phys. **2014**, 093B06 (2014).